1. Introduction

Because Mylonakis earth pressure equations (Mylonakis et al. (2007)) do not satisfy the equation of equilibrium, they can not be interpreted as theoretical "lower bound solutions." They may be lower bound, but we cannot know it theoretically. We only know it experimentally (or from experience). It is not appropriate to say it is "inherently" conservative. It is also not appropriate to say they are "solutions," because they are not solutions of any differential equations. There are three reasons why Mylonakis earth pressure equations do not satisfy the equation of equilibrium; one of them is explicitly stated in their paper, but two of them are not stated and it is difficult for the readers to notice. This document will explain why theoretical lower bound solutions must satisfy the equation of equilibrium and why Mylonakis earth pressure equations do not satisfy the equation of equilibrium.

2. Why theoretical lower bound solutions must satisfy the equation of equilibrium?

The lower bound theorem can be derived from the principle of virtual work. In the following, first, the principle of virtual work will be reviewed. Then the lower bound theorem will be reviewed.

2.1 The principle of virtual work

Assume a stress field σ_{ij} that satisfies the equation of equilibrium

$$\sigma_{ij,j} + \rho b_i = 0 \tag{1}$$

and a displacement field u_i that satisfies the equation of compatibility

$$\varepsilon_{ij} = \frac{1}{2} \left(u_{i,j} + u_{j,i} \right). \tag{2}$$

The stress field σ_{ij} and the displacement field u_i can be completely independent. We do not require that they are connected with a constitutive equation. Multiplying Equation (1) with u_i , integrating over a volume and applying Gauss's law yields

$$\int_{V} \rho b_{i} u_{i} dV = -\int_{V} \sigma_{ij,j} u_{i} dV = -\int_{V} \left(\sigma_{ij} u_{i}\right)_{,j} dV + \int_{V} \sigma_{ij} u_{i,j} dV$$

$$= -\int_{S} \sigma_{ij} u_{i} n_{j} dS + \int_{V} \sigma_{ij} u_{i,j} dV = -\int_{S} t_{i} u_{i} dS + \int_{V} \sigma_{ij} \varepsilon_{ij} dV. \tag{3}$$

For the final term, we used the Cauchy equation

$$t_i = \sigma_{ij} n_j \tag{4}$$

and the symmetry equation

$$\sigma_{ij} = \sigma_{ji}. (5)$$

From Equation (3) we obtain

$$\int_{S} t_{i} u_{i} dS + \int_{V} \rho b_{i} u_{i} dV = \int_{V} \sigma_{ij} \varepsilon_{ij} dV.$$
 (6)

Equation (6) is called the principle of virtual work. A similar relation can be established for a displacement rate field \dot{u}_i :

$$\int_{S} t_{i} \dot{u}_{i} dS + \int_{V} \rho b_{i} \dot{u}_{i} dV = \int_{V} \sigma_{ij} \dot{\varepsilon}_{ij} dV. \tag{7}$$

2.2 Lower bound theorem

Hill (1948) assumed that, for a plastic strain rate $\hat{\varepsilon}_{ij}^p$ defined at a point on a yield surface in a stress space, the rate of plastic work done by the stress σ_{ij} corresponding to this point is greater than or equal to the rate of plastic work done by any stress σ_{ij}^* within the yield surface:

$$\sigma_{ij}\dot{\varepsilon}_{ij}^p \ge \sigma_{ij}^*\dot{\varepsilon}_{ij}^p. \tag{8}$$

This is called the maximum plastic work principle. Figure 1 shows a conceptual diagram showing Hill's assumption. Hill's assumption holds if the material is convex and ε_{ij}^p follows the associated flow rule. From now on, let us assume that the material is convex.

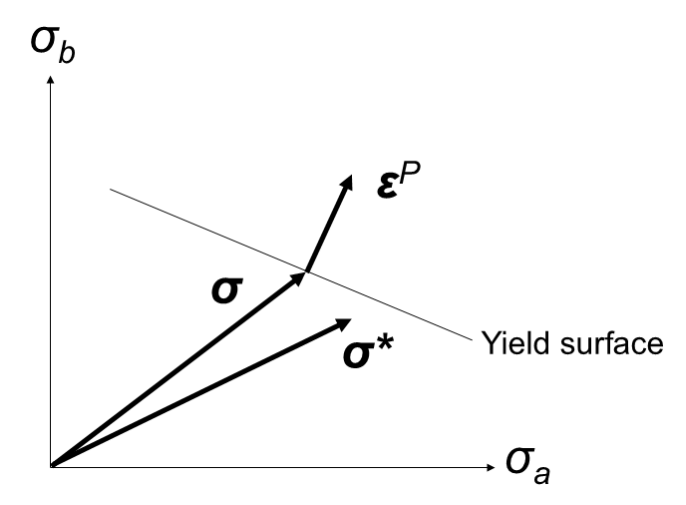


Figure 1 Conceptual diagram showing the Hill's assumption

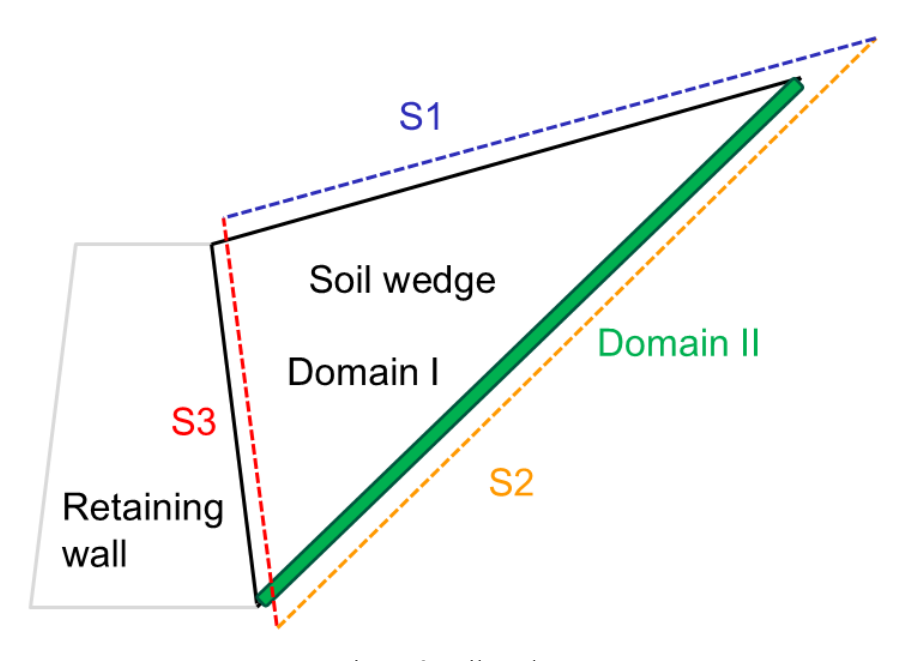


Figure 2 Soil wedge

Now let us consider a domain (e.g., a soil wedge as shown in Figure 2) with a stress field σ_{ij} and a plastic strain rate $\dot{\varepsilon}^p_{ij}$ and assume that the domain belongs to either of the following two domains: Domain I, where $\dot{\varepsilon}^p_{ij} = 0$ (if the material behaves as a rigid body, this applies)

Domain II, where the stress σ_{ij} is on the yield surface and $\dot{\varepsilon}_{ij}^p$ is related to σ_{ij} with the associated flow rule. In addition, let us consider another stress field σ_{ij}^* which satisfies the equation of equilibrium everywhere in the domain and within the yield surface. Then, Equation (8) holds everywhere in the domain. By integrating both sides of Equation (8) and applying Equation (7), we obtain

$$\int_{S} t_{i} \dot{u}_{i}^{p} dS \ge \int_{S} t_{i}^{*} \dot{u}_{i}^{p} dS \tag{9}$$

because the self-weight vanishes. The surface integral must be taken along S1, S2 and S3 (Figure 2). However, the traction vanishes for S1 and the displacement rate vanishes for S2. Consequently, the integral along S3 remains:

$$\int_{S3} t_i \dot{u}_i^p dS \ge \int_{S3} t_i^* \dot{u}_i^p dS. \tag{10}$$

This gives the lower bound theorem for the earth pressure. If we can come up with a stress field σ_{ij}^* which satisfies the equation of equilibrium everywhere in the domain and within the yield surface, the associated traction t_i^* gives the lower bound solution.

It should be noted that, for an active case, the traction vector and the displacement rate vector are pointing different directions. Therefore, the absolute value of the earth pressure is smaller than the lower bound solution. For a passive case, the opposite applies.

In conclusion, for a lower bound solution, the stress field σ_{ij}^* must satisfy the equation of equilibrium everywhere in the domain.

3. Why Mylonakis earth pressure equations do not satisfy the equation of equilibrium?

The remainder of the document will explain why Mylonakis earth pressure equations do not satisfy the equation of equilibrium. To begin with, the Kötter equations will be reviewed.

3.1 Kötter equations

In the remainder, the convention changes from "tension positive" to "compression positive", that is, σ and τ are positive if they are acting in the direction shown in Figure 3. In Figure 3, σ_1 and σ_3 are principal stresses ($\sigma_1 > \sigma_3$). If we consider the equilibrium of the element, we can obtain the following equations:

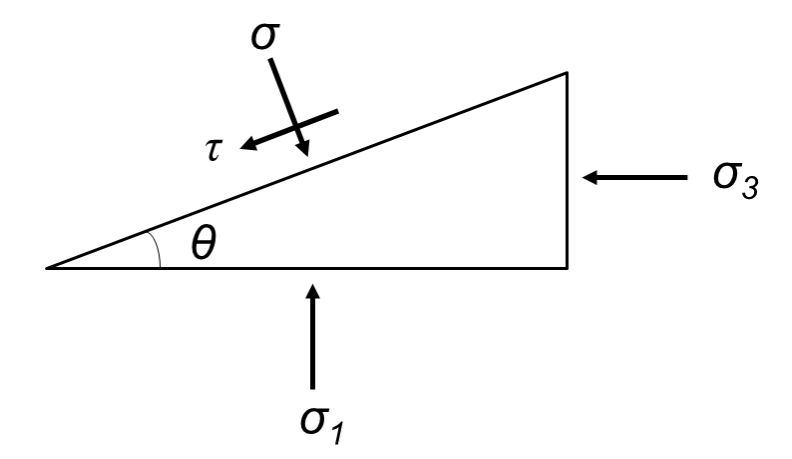


Figure 3 Sign convention (σ and τ are positive if they are acting in this direction)

$$\sigma = \frac{\sigma_1 + \sigma_3}{2} + \frac{\sigma_1 - \sigma_3}{2} \cos 2\theta$$

$$\tau = \frac{\sigma_1 - \sigma_3}{2} \sin 2\theta$$
(11)

or

$$\sigma = p + q\cos 2\theta \tag{13}$$

$$\tau = q \sin 2\theta \tag{14}$$

with

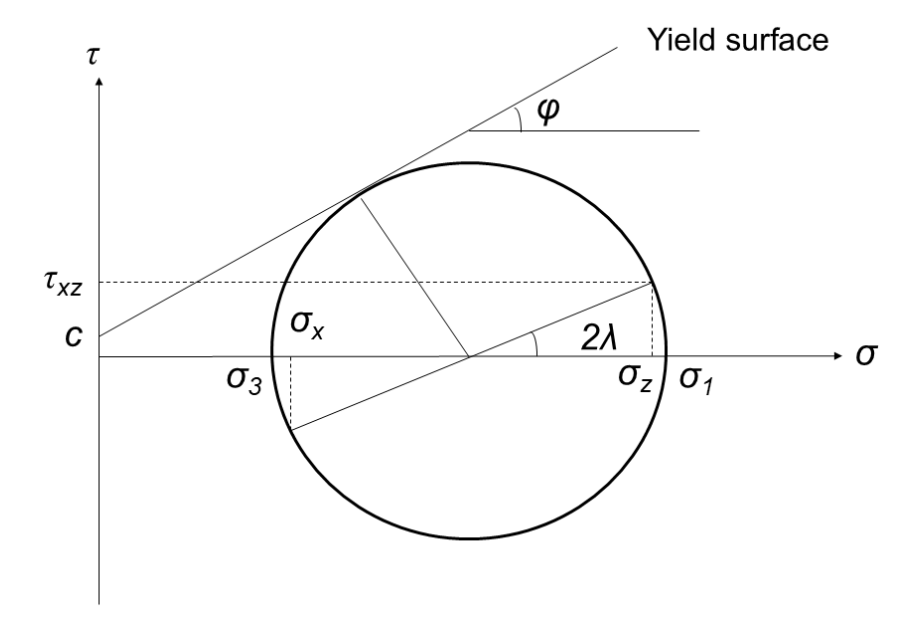
$$p = \frac{\sigma_1 + \sigma_3}{2}$$

$$q = \frac{\sigma_1 - \sigma_3}{2}$$
(15)

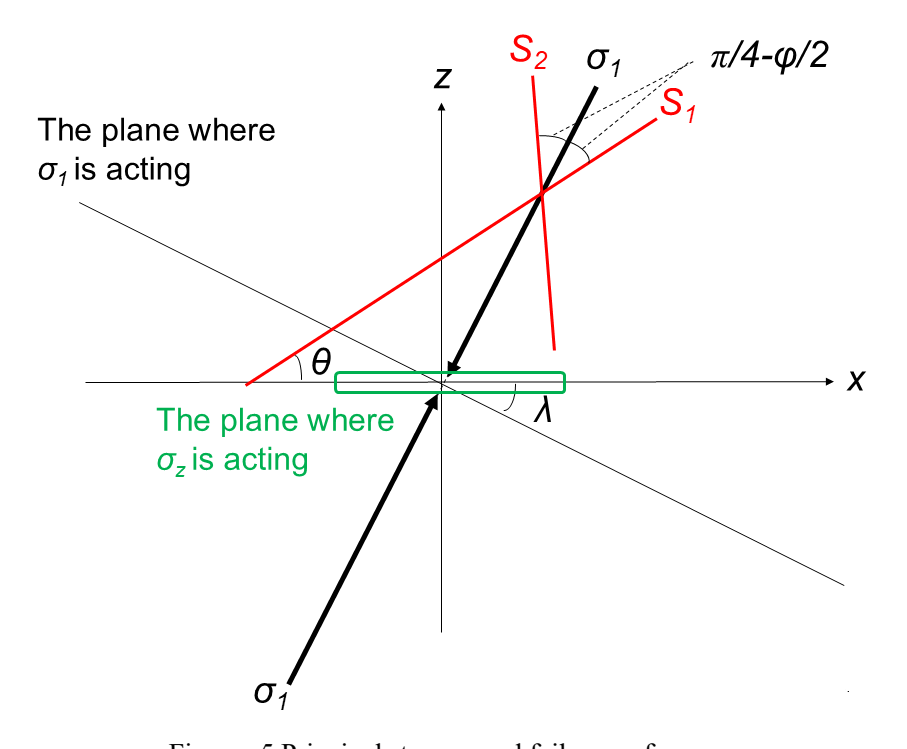
$$q = \frac{\sigma_1 - \sigma_3}{2} \tag{16}$$

Let us consider a domain in the soil in which the stress field satisfies the equation of equilibrium and the Mohr circle touches the yield surface everywhere as shown in Figures 4 and 5. In Figure 5, z denotes the vertical axis. The major principal stress σ_1 is acting on a plane which is rotated clockwise by an angle of λ from the plane where σ_z is acting. The failure surfaces S_1 and S_2 are rotated clockwise and counterclockwise, respectively, from the direction of σ_1 by an angle of $\pi/4 - \phi/2$. The angle between S_1 and the x axis is denoted by θ . From these configurations, we have:

$$\lambda = \frac{\pi}{4} - \theta + \frac{\phi}{2} \tag{17}$$



Figures 4 Mohr's circle



Figures 5 Principal stresses and failure surfaces

and

$$\sigma_{x} = p - q\cos 2\lambda \tag{18}$$

$$\sigma_z = p + q\cos 2\lambda \tag{19}$$

$$\tau_{xz} = q \sin 2\lambda. \tag{20}$$

It should be noted that λ and θ can be functions of x and z.

Because the stress field satisfies the equation of equilibrium and the Mohr circle touches the yield surface everywhere, we have:

$$\frac{\partial \sigma_x}{\partial x} + \frac{\partial \tau_{xz}}{\partial z} = 0 \tag{21}$$

$$\frac{\partial \tau_{xz}}{\partial x} + \frac{\partial \sigma_z}{\partial z} = -\gamma \tag{22}$$

$$q = c\cos\phi + p\sin\phi,\tag{23}$$

where γ denotes the unit weight. From now on, we will obtain differential equations in terms of p and θ . Using Equations (18) – (20) and using

$$\cos 2\lambda = \sin(2\theta - \phi) \tag{24}$$

$$\sin 2\lambda = \cos(2\theta - \phi) \tag{25}$$

we obtain

$$\sigma_x = p(1 - \sin\phi\sin(2\theta - \phi)) - c\cos\phi\sin(2\theta - \phi) \tag{26}$$

$$\sigma_z = p(1 + \sin\phi \sin(2\theta - \phi)) + c\cos\phi \sin(2\theta - \phi) \tag{27}$$

$$\tau_{xz} = (c\cos\phi + p\sin\phi)\cos(2\theta - \phi). \tag{28}$$

Substituting Equations (26) – (28) into Equations (21) – (22) yields

$$(1-\sin\phi\sin(2\theta-\phi))\frac{\partial p}{\partial x}-2(c\cos\phi+p\sin\phi)\cos(2\theta-\phi)\frac{\partial\theta}{\partial x}$$

$$+\sin\phi\cos(2\theta-\phi)\frac{\partial p}{\partial z}-2(c\cos\phi+p\sin\phi)\sin(2\theta-\phi)\frac{\partial\theta}{\partial z}=0$$
 (29)

$$\sin\phi\cos(2\theta-\phi)\frac{\partial p}{\partial x}-2(c\cos\phi+p\sin\phi)\sin(2\theta-\phi)\frac{\partial\theta}{\partial x}$$

$$+(1+\sin\phi\sin(2\theta-\phi))\frac{\partial p}{\partial z}+2(c\cos\phi+p\sin\phi)\cos(2\theta-\phi)\frac{\partial\theta}{\partial z}=-\gamma \qquad (30)$$

From now on, we will introduce curvilinear coordinates s_1 and s_2 along the failure surfaces s_1 and s_2 (both upward positive). The relations between the coordinates are

$$\frac{\partial}{\partial s_1} = \cos\theta \, \frac{\partial}{\partial x} + \sin\theta \, \frac{\partial}{\partial z} \tag{31}$$

$$\frac{\partial}{\partial s_2} = -\sin(\theta - \phi)\frac{\partial}{\partial x} + \cos(\theta - \phi)\frac{\partial}{\partial z}$$
 (32)

which is equivalent to

$$\frac{\partial}{\partial x} = \frac{1}{\cos \phi} \left(\cos(\theta - \phi) \frac{\partial}{\partial s_1} - \sin \theta \frac{\partial}{\partial s_2} \right)$$
 (33)

$$\frac{\partial}{\partial z} = \frac{1}{\cos \phi} \left(\sin(\theta - \phi) \frac{\partial}{\partial s_1} + \cos \theta \frac{\partial}{\partial s_2} \right). \tag{34}$$

Applying Equations (33) - (34) into Equations (29) - (30) yields

$$(\cos(\theta - \phi) - \sin\phi\sin\theta)\frac{\partial p}{\partial s_1} - 2(c\cos\phi + p\sin\phi)\cos\theta\frac{\partial\theta}{\partial s_1}$$

$$+(-\sin\theta + \sin\phi\cos(\theta - \phi))\frac{\partial p}{\partial s_2} - 2(c\cos\phi + p\sin\phi)\sin(\theta - \phi)\frac{\partial \theta}{\partial s_2} = 0$$
 (35)

$$(\sin(\theta - \phi) + \sin\phi\cos\theta)\frac{\partial p}{\partial s_1} - 2(c\cos\phi + p\sin\phi)\sin\theta\frac{\partial\theta}{\partial s_1}$$

$$+(\cos\theta + \sin\phi\sin(\theta - \phi))\frac{\partial p}{\partial s_2} + 2(\cos\phi + p\sin\phi)\cos(\theta - \phi)\frac{\partial\theta}{\partial s_2} = -\gamma\cos\phi \qquad (36)$$

From equations (35) and (36) we obtain the Kötter equations:

$$\cos\phi \frac{\partial p}{\partial s_1} - 2(c\cos\phi + p\sin\phi) \frac{\partial \theta}{\partial s_1} = -\gamma\sin(\theta - \phi)$$
 (37)

$$\cos\phi \frac{\partial p}{\partial s_2} + 2(c\cos\phi + p\sin\phi) \frac{\partial \theta}{\partial s_2} = -\gamma\cos\theta. \tag{38}$$

It should be noted that there are two equations.

3.2 Logarithmic stress fan

Let us consider Kötter equations for c = 0 and $\gamma = 0$:

$$\cos\phi \frac{\partial p}{\partial s_1} - 2p\sin\phi \frac{\partial \theta}{\partial s_1} = 0 \tag{39}$$

$$\cos\phi \frac{\partial p}{\partial s_2} + 2p\sin\phi \frac{\partial \theta}{\partial s_2} = 0. \tag{40}$$

Let us assume that the direction of s_1 rotates with β as shown in Figure 6:

$$\theta = \theta_0 + \beta. \tag{41}$$

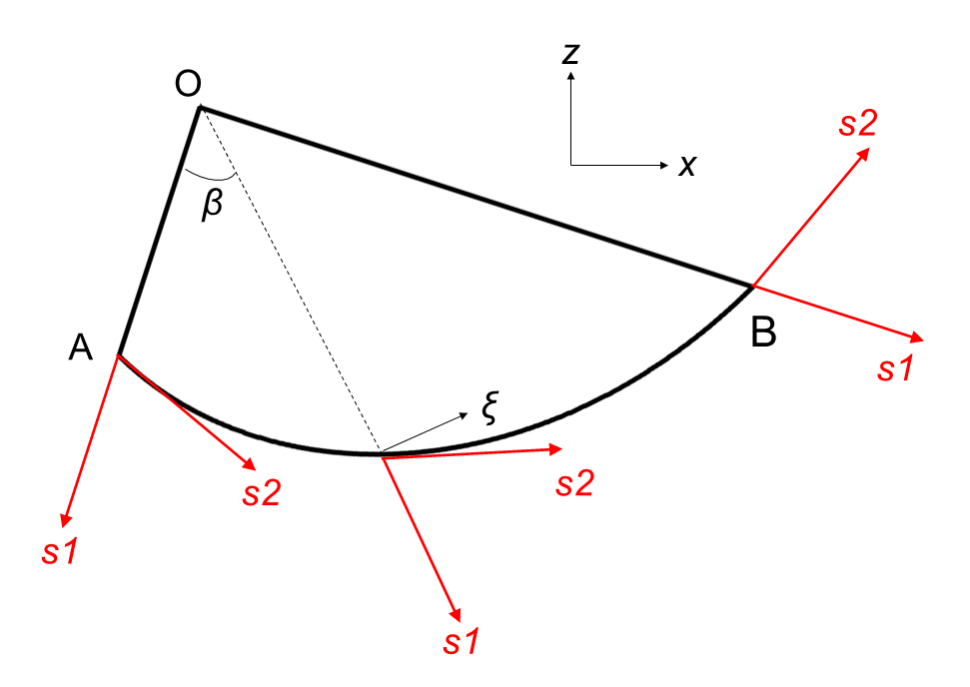


Figure 6 Logarithmic stress fan

The direction of the principal axis rotates accordingly. In this case, the logarithmic spiral expressed as

$$r = r_0 e^{\beta \tan \phi} \tag{42}$$

can reside along the s_2 axis and can be a candidate for a failure surface. This can be shown as follows. If we consider a small increment $d\beta$ at an arbitrary point on the spiral, the increment of the distance from O is

$$dr = \frac{dr}{d\beta}d\beta = \tan\phi \, r_0 e^{\beta \tan\phi} d\beta = \tan\phi \, r d\beta. \tag{43}$$

On the other hand, the increment of the coordinate ξ (shown in Figure 6) is $rd\beta$. Therefore, the angle between the spiral and the ξ axis is ϕ . Therefore, the angle between the spiral and the s_1 axis is $\pi/2 - \phi$, which shows that the spiral is parallel to the s_2 axis.

Let us go back to the Kötter equations. Noting that

$$ds_2 = \frac{d\xi}{\sin\phi} = \frac{r}{\sin\phi} d\beta \tag{44}$$

the latter of the two Kötter equations, Equation (40), can be written as

$$\cos\phi \frac{\partial p}{\partial \beta} + 2p\sin\phi = 0. \tag{45}$$

This constitutes a differential equation which must be satisfied by the mean stress p. The solution is

$$p = p_0 e^{-2\beta \tan \phi}. (46)$$

This means that, for the failure to actually occur along the spiral, the mean stress p must change along the spiral as a function of β as shown in Equation (46). This condition is considered in the Mylonakis equations (Equation (8) in Mylonakis et al. (2007)). However, the former of the two Kötter equations, Equation (39), is not considered in their paper. Another fact to be noted here is that, in the logarithmic stress fan, the amount of principal axis rotation between A and B equals to the angle AOB.

3.3 There is no space for the "fan"

In the Mylonakis equations, Zone A (near the surface) and Zone B (near the wall) are in different stress statuses (Figure 7) and they are connected with the logarithmic stress fan. However, they did not mention where is the boundary between the zones and the fan. In addition, they did not mention where they evaluated the mean stress in Zone A (in their notation, S_A). According to my study, S_A was evaluated just behind the wall (the red circle in Figure 7).

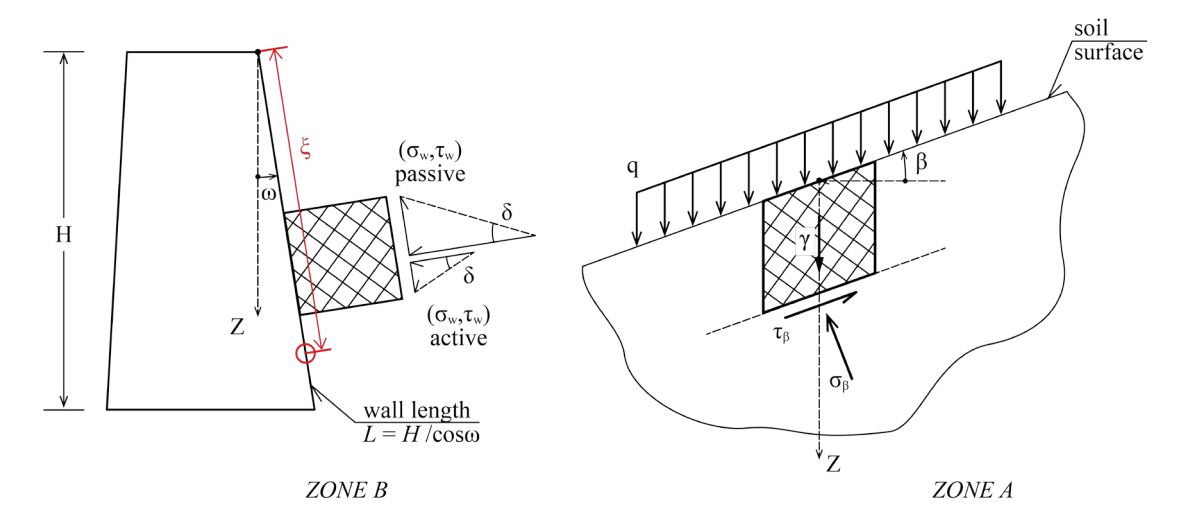


Figure 7 Zone A (near the surface) and Zone B (near the wall)

$$\sigma_{\beta} \to S_A \to S_B \to \sigma_{\omega}$$

Figure 8 Steps to evaluate σ_{ω}

Figure 8 shows the steps to evaluate σ_{ω} in Mylonakis et al. (2007). From left to right, Equations (5) (10) and (8) in their paper are used. The depth of the red circle from the surface can be evaluated as

$$depth = \xi \sin \omega \tan \beta + \xi \cos \omega = \xi \frac{\sin \omega \sin \beta + \cos \omega \cos \beta}{\cos \beta} = \xi \frac{\cos(\omega - \beta)}{\cos \beta}.$$
 (47)

From this equation and Equation (4a) in Mylonakis et al. (2007), we have

$$\sigma_{\beta} = \gamma \cdot depth \cdot \cos^2 \beta = \gamma \xi \cos(\omega - \beta) \cos \beta. \tag{48}$$

From this equation and Equations (5) (10) and (8) in Mylonakis et al. (2007), we have

$$\sigma_{\omega} = \gamma \xi \cos(\omega - \beta) \cos \beta \left[\frac{1 \mp \sin \phi \cos(\Delta_2 \mp \delta)}{1 \pm \sin \phi \cos(\Delta_1 \pm \beta)} \right] \exp(\mp 2\theta \tan \phi). \tag{49}$$

Integrating along the soil-wall interface yields

$$P = \frac{1}{\cos \delta} \int_0^{H/\cos \omega} \sigma_{\omega} d\xi = \frac{1}{2} \frac{\cos(\omega - \beta) \cos \beta}{\cos \delta \cos^2 \omega} \left[\frac{1 + \sin \phi \cos(\Delta_2 + \delta)}{1 + \sin \phi \cos(\Delta_1 + \beta)} \right] \exp(\pm 2\theta \tan \phi) \gamma H^2.$$
 (50)

Comparing this equation with Equation (11) in their paper, we obtain

$$K_{\gamma} = \frac{\cos(\omega - \beta)\cos\beta}{\cos\delta\cos^{2}\omega} \left[\frac{1 + \sin\phi\cos(\Delta_{2} + \delta)}{1 + \sin\phi\cos(\Delta_{1} + \beta)} \right] \exp(\pm 2\theta \tan\phi). \tag{51}$$

This equation coincides with Equation (12) in their paper.

In conclusion, the stress status in Zone A is evaluated just behind the wall (the red circle in Figure 7). There is no space for the fan. Zones with different stress statuses are directly connected. Therefore, the stress field in Mylonakis et al. (2007) cannot satisfy the equation of equilibrium.

3.4 Failure to satisfy one of the two Kötter equations

Equations (5) in their paper follows the latter of the two Kötter equations, Equation (40). However, the stress field does not satisfy the former of the two Kötter equations, Equation (39). In fact, in their stress field, the direction of the principal stress is fixed along the s_1 axis, at least at the boundaries $(\partial\theta/\partial s_1=0)$. However, the mean stress changes linearly (p.965 of their paper) $(\partial p/\partial s_1\neq 0)$. Therefore, one of the two Kötter equations is not satisfied. This is the second reason why the stress field in Mylonakis et al. (2007) cannot satisfy the equation of equilibrium.

3.5 Neglection of gravity acting on the "fan"

Equations (5) in their paper follows Equation (40) in this document, which does not consider the unit weight of the soil in the fan. This is the third reason why the stress field in Mylonakis et al. (2007) cannot satisfy the equation of equilibrium. This fact is explicitly mentioned in Mylonakis et al. (2007).

4. Conclusion

The conclusion was already written at the beginning of this document.

Reference

Hill (1948): A variational principle of maximum plastic work in classical plasticity, *Quarterly Journal of Mechanics and Applied Mathematics*, Vol.1, pp.18-28.

Mylonakis, G., Kloukinas, P. and Papantonopoulos, C. (2007): An alternative to the Mononobe-Okabe equations for seismic earth pressures, *Soil Dynamics and Earthquake Engineering*, Vol.27, pp.957-969.